CONF-860501--10

DEFORM-4: Fuel Pin Characterization and Transient Response in the SAS4A Accident Analysis Code System*

K. J. Miles
Nuclear Engineer

D. J. Hill
Nuclear Engineer

Reactor Analysis and Safety Division
Argonne National Laboratory
Argonne, IL 60439, U.S.A.

CONF-860501--10

DE86 012118

DISCLAIMER

*Work supported by the U.S. Department of Energy, Breeder Reactor Programs under Contract W-31-109-Eng-38

The DEFORM-4 module is the segment of the SAS4A Accident Analysis Code System that calculates the fuel pin characterization in response to a steady state irradiation history, thereby providing the initial conditions for the transient calculation. The various phenomena considered include fuel porosity migration, fission gas bubble induced swelling, fuel cracking and healing, fission gas release, cladding swelling, and the thermal-mechanical state of the fuel and cladding. In the transient state, the module continues the thermal-mechanical response calculation, including fuel melting and central cavity pressurization, until cladding failure is predicted and one of the failed fuel modules is initiated. Comparisons with experimental data have demonstrated the validity of the modeling approach.

INTRODUCTION

1. The response of LMFBR fuel pins to transient accident conditions is an important safety concern. For transients leading to pin failure, the failure modes and initial fuel disruption depend in part on pre-transient irradiation effects, such as restructuring, fission-gas retention, fuel-cladding gap, central void size and makeup. As the transient fuel-pin models develop, an increasingly rigorous pre-transient fuel-pin characterization of the fuel pin is also required. For this reason, an effort has been made to integrate a detailed treatment of the pre-transient fuel-pin characterization into SAS4A. At the same time, an attempt has been made to assure that the models are consistent with the transient calculation and, where possible, to develop models in such a manner that they can be used in both the pre-transient and transient calculations.

2. Because the phenomena affecting fuel-pin integrity are not all well understood, most performance codes use one of two methods to predict the pin characterization: (1) empirical correlations derived from a data base of experimentally determined information, or (2) a phenomenological description of the process that contains parameters that need to be calibrated to experiments or the information data base. Care must be exercised with both approaches, but especially with the former method, because unrealistic values can be obtained if the pin conditions fall outside the correlation data base. In the phenomenological (or mechanistic) approach the attempt is made to model the physical process taking place and then calibrate this to available data. Since the model attempts to describe the physical processes, it is possible to extrapolate the response to conditions outside the calibration data base with greater assurance than with the correlation approach. It was, therefore, decided that this mechanistic approach would be adopted wherever possible in the DEFORM-4 module of SAS4A.

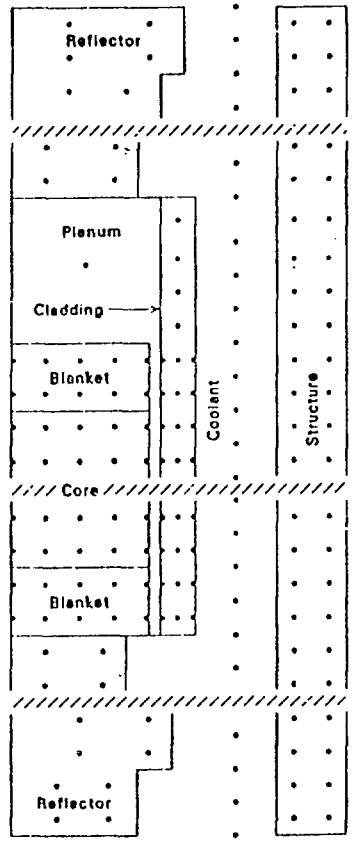

Fig. 1. SAS4A/DEFORM-4 Node Structure

3. The pin is divided into a number of axial segments ($\leq$ 24) of arbitrary length. The fuel and cladding are assumed to occupy the same axial segment. Figure 1 shows an example of the axial and radial discretization for a fuel pin with an upper fission-gas plenum. The DEFORM-4

module is concerned with the axial region containing the driver fuel, axial blankets, and the fission-gas plenum. There are three fuel-cladding gap conditions considered: (1) no contact between the fuel and cladding, (2) the fuel elastically straining the cladding, and (3) the fuel plastically straining the cladding. A central cavity may form in the hotter regions of the driver fuel.

4. The fuel in an axial segment is divided into a series of radial cells (Fig. 1). The radial cell boundaries may be determined on the basis of equal mass in each, except the inner and outer cells which contain half the mass of a regular cell, or with each cell thickness being equal, again except for the inner and outer cell which have half the nominal thickness. The cladding is divided into two radial cells.

5. The fuel pin is divided radially into six radial zones of different characteristics. Not all zones may exist and each that does may contain one or more radial cells. These zones are (1) the central void, (2) the molten fuel, (3) the solid, continuous fuel, (4) the cracked fuel, (5) the fuel-cladding gap, and (6) the cladding. These zones are illustrated in Fig. 2.

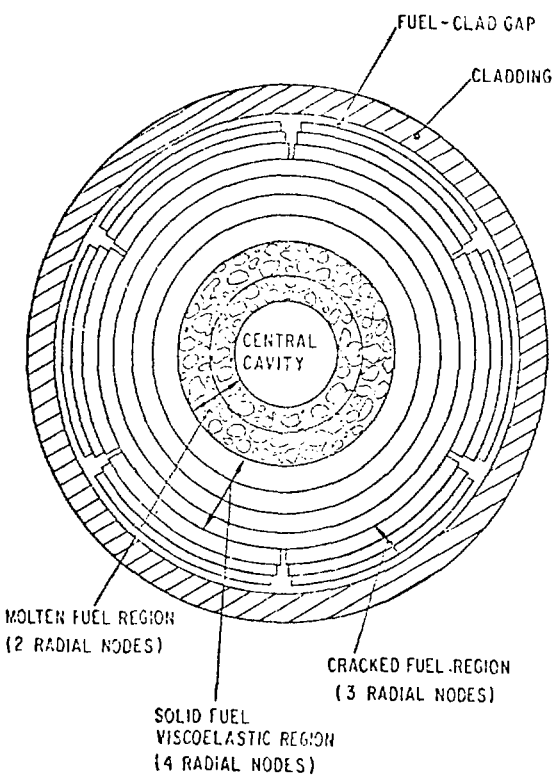

Fig. 2. DEFORM-4 Radial Zones

FUEL PIN MECHANICS

6. The mechanics calculation is divided into three areas that are added together to obtain the total strain in the fuel or cladding cells. The thermal expansion induced strains and stresses are determined and added to those from the elastic response to the boundary conditions. To this is then added the strains resulting from the plastic deformation resulting from fuel swelling, stress induced plastic creep of the cladding, and irradiation induced swelling of the cladding.

Solid Fuel and Cladding

7. The solid fuel and cladding is assumed to be continuous, isotropic, elastic, and axisymmetric. Because of the axisymmetry, all shear stresses and strains are assumed to be zero. The generalization of Hooke's Law to three dimensions is used to provide the linear elastic relationship between the stresses and strains. The thermal expansion strains are included through the principle of superposition of linear equations. The strains are related to the displacements through geometrical considerations. In order to be able to obtain simple analytical solutions a generalized plane strain approximation has been employed. Each axial segment is assumed to elongate uniformly over the cross section to maintain a plane interface between segments. Since the cells under consideration are assumed to be at rest, with no shear stresses, mechanical considerations provide the equation of equilibrium.

8. The temperature changes over the time step are received from the thermal calculations of SAS4A. These and the material properties at these temperatures determine the thermal expansion. The boundary conditions are the pressure in the central cavity and the fuel-cladding interface pressure, for the fuel. For the cladding they are the fuel-cladding interface pressure and the coolant channel pressure, as well as the temperature changes. The interface pressure is the major variable determined during the solution procedure. As the outer fuel and inner cladding radii are determined from the displacements calculated, the interface pressure is adjusted to provide a match between the fuel and cladding surfaces, if the gap is closed.

Cracked Fuel

9. If the circumferential stress at a cell boundary exceeds the fracture strength of the fuel, the cell immediately inside that boundary is assumed to crack. The new outer solid fuel boundary is then studied to determine if it will also crack. This processes is repeated until a stable solid boundary is reached, or cracking occurs to the central void or molten fuel boundary.

10. In the cracked zone, it is assumed that numerous radial and transverse cracks exist and extend inward to the same radial position. Under these conditions the circumferential and axial stress, are both set equal to the negative of the plenum gas pressure, since it is assumed that communication exists with the plenum. If these values are substituted into the equilibrium equation, and the integration performed

from the outer fuel radius to an inner radius, the radial stress at any point in the cracked region results.

11. As the dimensions of a cracked fuel cell change, so will the fraction of the volume which is associated with the cracks. In the current version of DEFORM-4, the volume associated with transverse, or axial, cracking is neglected. The radial crack volume fraction is affected by three factors: (1) changes in the cell boundary locations, (2) circumferential strain, and (3) fission-product-induced fuel swelling.

Axial Expansion

12. The analytical solution to the mechanics equations is produced through a generalized plane strain assumption. The axial interfaces between segments are assumed to remain parallel, and a segment expands or contracts with a uniform strain, over its entire radius. Since this axial strain exists in the equations which represent the radial displacement function, it is necessary to find the axial strain prior to the radial strain results.

13. In order to find the axial plane strain, a total force balance is performed. The state of the fuel-cladding gap can influence the terms in the force summation. If the fuel-cladding gap is open, or the free axial expansion option is chosen through the input parameters, then the force summation contains no term for the cladding effects. If, however, the fuel and cladding are in contact, then cladding terms must be included in the force balance.

14. The axial strain is separated into its thermal and force components to allow for the option to use only thermal effects or both thermal and force effects through input parameters. There are also four options available which concern the treatment of the fuel-cladding locking. The axial expansion can be set to the free axial expansion of the fuel, to free expansion of the cladding, to always be constrained expansion, or to be a combination depending on the actual interface conditions. In the fourth option, all axial segments below the top locked segment are assumed to be in the constrained state. These options are controlled through the input parameters. The most realistic options are both thermal and force components with the mixed free/constrained state. The other options are available to facilitate the study of axial expansion assumptions on accident sequences.

PHENOMENOLOGICAL MODELS

15. All phenomenological models contained in DEFORM-4 are coded so that they may be used in both the pre-transient and transient phase. The inclusion of a model in the pre-transient phase is a function of the time scale of the phenomenon, not a limitation of the coding. Those that require hours or days to cause changes in structure or properties are not included in the transient phase of the calculation.

As-Fabricated Porosity Migration

16. When cylindrical oxide fuel pins are placed in a neutron flux, the volumetric heating rates and low thermal conductivity of the fuel combine to produce high temperatures and very steep radial thermal gradients. These conditions can lead to the phenomenon commonly referred to as restructuring. The most distinct macroscopic aspects are divided into the columnar, equiaxed, and as-fabricated fuel zones. The basic physical processes that produce these zones have been identified as grain growth kinetics for the equiaxed zone, and porosity migration for the columnar zone.

17. Sintered fuel pellets contain residual pores on the grain boundaries. At the high temperatures commonly experienced in a nuclear fuel pin, the mobility of the constituent atoms can become important since this activity is usually related to the internal energy, which is represented in an Arrhenius equation form. However, if the temperature was uniform, there would be no macroscopic movement because there is no driving force. The large thermal gradients that exist in a fuel pin act as the driving force for atomic movement. This mobility and driving force cause the pores to migrate up the thermal gradient. This movement of porosity is important because the thermal conductivity of the fuel depends on its local porosity. If there is a large amount of pore migration a central hole will be formed. This change in geometry affects the heat-transfer characteristics of the pin.

18. In DEFORM-4 the pore velocity is represented by an Arrhenius term divided by temperature to represent a combined evaporation-condensation and surface diffusion process. These velocities are evaluated at the radial cell boundaries, which determines the porosity entering and leaving the cells. These adjustments are made to the cell porosity and a new cell volume determined. The columnar grain boundary is determined as the boundary the porosity is an input fraction of the original porosity.

Grain Growth

19. At the relatively low temperatures in the outer fuel region, the as-fabricated porosity is unable to migrate despite the large thermal gradient, because the atomic mobility is too low. However, the atoms may be active enough to cross the grain boundaries. The larger grains grow at the expense of the smaller, due to the tendency of atoms to jump from a convex (higher energy) to a concave (lower energy) surface. The net effect is to reduce the surface area, and thereby, the surface energy associated with the grains. This grain growth is a strong function of atomic activity, i.e., temperature. In nuclear fuels, the surface temperature is usually below the "threshold" temperature where activity is great enough to cause redistribution at the grain surfaces. Due to the strong temperature dependence and the steep thermal gradient, a distinct region usually develops where the grains grow isotropically, irrespective of the large gradient. This "equiaxed" zone extends inward to the region where pore migration becomes active and produces the "columnar" grains by dragging the boundaries during migration.

20. The grain-size distribution is important because the fission-gas release and fuel-creep

functions depend on this parameter. The calculation of this clearly visible zone also offers a simple experimental calibration region which can be used in the validation process.

21. Two grain-growth models are available in the DEFORM-4: unlimited grain-growth and a limited grain-growth model. In this latter model the grain sizes are limited to an experimentally determined value. Both models give very similar results in the lower temperature regions associated with the equiaxed region where the grains are usually two to ten times the initial size. At higher temperatures, the first model results in larger grains because of the unconstrained growth. However, in these regions, porosity migration also produces the columnar grain structure which uses a separate method for determining the effective grain size for use in the fission-gas release and fuel-creep calculations.

Fission-Gas Release

22. The nuclear fission processes occurring in the fuel during the irradiation produce both solid and gaseous fission products. The gaseous products are primarily xenon and krypton. The model currently used in DEFORM-4 assumes that the gaseous products either precipitate as gas-filled bubbles on the grain boundaries, are contained in microbubbles within the fuel matrix, or are released to the available free volume in the pin plenum and fuel central void. Formation of grain boundary bubbles leads to fuel swelling and reduces the fuel-cladding gap size. The intra-granular gas is assumed to play no part in fuel swelling but becomes important upon fuel melting. Release to the free volume changes the gas mixture and reduces the thermal conductivity of the gas in the gap. Fission-gas release, fuel swelling, and the fuel-pin temperature distribution are therefore closely interrelated. The migration of fission-gas bubbles up the thermal gradient is not treated.

23. Because of the need to carry out a large number of calculations over multiple axial and radial nodes in several channels, DEFORM-4 does not attempt to provide a detailed gas release calculation but uses a basic rate equation with a fractional release rate. Because the mobility of gas atoms within the fuel matrix is a thermally activated process, this release rate is defined as an Arrhenius relationship which is calibrated to experimental data. This rate equation is solved for each axial and radial node providing a fission gas release map for the fuel pin.

Fuel Swelling

24. In DEFORM-4, the as-fabricated porosity and the fission-gas-generated porosity are treated separately. The migration of the as-fabricated porosity can lead to either densification or swelling of the fuel depending on local conditions. The newly formed porosity arising from fission-gas bubbles introduces additional porosity that may be in a nonequilibrium condition, depending on the amount of gas in the bubbles, the local hydrostatic pressure, and the fuel surface tension. This fission-gas porosity may increase or decrease as a function of time, producing changes in the fuel dimensions through swelling or densification. These changes in fuel porosity also affect the fuel thermal conductivity, since both the as-fabricated and fission-gas porosity are considered in the porosity terms. In addition to this gas effect, the solid fission products locate themselves interstitially in the fuel matrix, causing strains that produce swelling. Both these effects are accounted for by DEFORM-4.

25. Swelling strains may occur both axially and radially. In general, the axial swelling strains in oxide fuels are relatively small compared to the thermal expansion effects. However, in some transients the differences caused by including the axial swelling can be enough to modify the accident scenario. For this reason, and to provide the basis for future versatility, axial swelling has been incorporated into DEFORM-4. Radial swelling is important because of the effects on fuel-cladding gap size and mechanical interaction. Both effects can produce large differences in the prediction of cladding failure, so radial swelling is also included in DEFORM-4.

26. The swelling rate due to fission gas depends on the release of the gas to grain boundaries and formation of fission-gas bubbles. While fission gas exists in both the fuel matrix and on grain boundaries, it is the bubbles on the grain boundaries that produce the significant swelling in oxide fuels. If these bubbles are underpressurized, a reduction in the bubble volume due to the fuel hydrostatic pressure will reduce the volume of a fuel cell. If the bubbles are overpressurized, an increase in bubble size, and thereby fuel cell volume can result. To determine the rate of swelling, or densification, the mechanical stresses, internal gas pressure, pressure due to surface tension, and the creep properties of the fuel must be known.

27. The swelling rate of the bubbles is estimated from the fuel creep function. Swelling causes changes in the stress state of the fuel because the changes in geometry produce changes in the boundary conditions. But changes in stress states also produce changes in the swelling through changes in hydrostatic pressures. The swelling and mechanical response are closely coupled. For this reason, the swelling calculation in DEFORM-4 has been incorporated within the iterations to find the set of conditions that bring about consistency between the fuel and cladding. Swelling and mechanical strains are stored separately, but calculated considering mutual influences. The strains due to swelling/hot pressing of the fuel are added to the total mechanical deformation at the end of each time step.

28. In addition to the gaseous fission-product swelling, there is solid fission-product swelling from products such as zirconium, niobium, molybdenum, the rare earths, yttrium, etc. A detailed treatment of these solid fission products, which considered their physical and chemical state to determine the partial volumes, would yield the lattice strain cre-

ated. This, together with the isotopic yields from fission, would result in a mechanistic estimate of solid product swelling. This type of treatment requires more computational resources than are warranted for the magnitude of the phenomenon. A simpler model is assumed which relates the fractional volume change to the fuel burnup.

29. The volume changes from solid product changes are included with those of the volatile products when determining the changes in fuel volume that may change the fuel-cladding interface conditions. However, this volume change is not affected by the local hydrostatic pressure and therefore remains a constant through the iterations mentioned above.

Irradiation-Induced Cladding Swelling

30. When cladding materials are irradiated in a fast neutron flux, there may be a temperature- and flux-dependent reduction in density through the formation of irradiation-induced voids. The model in DEFORM-4 is based on an empirical correlation corresponding to stress-free swelling. The correlation represents two characteristics of irradiation-induced swelling based on experimental findings. First, the rate of swelling the cladding is temperature sensitive. Second, there appears to be an incubation period during which little change in density is observed. The swelling is assumed to be isotropic and always outward. The new cross sectional area is calculated assuming 1/3 of the volume change takes place axially. The rest takes place radially.

FISSION-GAS PLENUM PRESSURE

31. As the volatile fission products are released from the fuel, it enters the free volume associated with the fuel pin and is assumed to mix homogeneously with the gases already present. The free volumes considered are the fabricated fission gas plenum, the central fuel void not associated with a central molten fuel cavity, the fuel-cladding gap, and the crack volume within the fuel. A homogeneous ideal-gas mixture that is in pressure equilibrium is assumed to form.

32. The amount of helium is known from the fill gas pressure, the fraction that is not helium, and the reference temperature geometry. The amount of helium also contains the amount released as porosity migration occurs. The number of moles of fission gas is known from the fission gas release calculation and the non-helium initial fill gas.

MOLTEN CAVITY PRESSURIZATION

33. Prior to fuel melting, the central void and plenum are assumed to be in pressure equilibrium. Once melting has begun, DEFORM-4 provides for three different methods for calculating the molten cavity pressure: (1) the cavity under consideration extends axially only over the range of segments where melting has occurred, (2) the cavity extends over all axial segments, and (3) each axial segment is considered a separate cavity.

34. If a central void exists before fuel melting, then the first two options give similar results. The second option presents a more mechanistic approach to the molten cavity. As melting begins, it is expected that communication would exist all along the central void. As the available volume for the helium and fission gas associated with one axial segment is decreased because of fuel melting and thermal expansion, the excess gas would move to other segments to produce a balanced pressure all along the central void. This model assumes that the transient time scales are long enough to allow this redistribution process.

35. The third option is included for the study of extremely fast transients. If the time scale is short enough to preclude material redistribution, then each axial segment is assumed to act as a separate molten cavity. A separate pressure is calculated for each segment, and axial pressure differentials are produced. The effects of these axial differentials on the radial mechanics solution in the cladding can then be studied to determine the sensitivity of cladding failure location.

36. In addition to these options, the effects of fuel moving into the cracks and pressurizing them to the same level as the molten cavity can be studied. In this case, the crack volume is included in the molten cavity volume and the cavity pressure acts directly on the cladding. Because DEFORM-4 does not consider mass transport between axial segments or radial cells, the actual movement of fuel cannot take place. The consideration of the crack volume does allow the macroscopic effect of volume increase in the molten cavity by movement of molten fuel out of the cavity into crack volume to be considered.

37. The radial extent of the molten cavity is determined by the relationship between the radial cell temperature and the solidus temperature. Melting of the cell is assumed to begin when the solidus temperature is reached, and be complete when the liquidus temperature is attained.

Gas and Volume Additions to Cavity

38. When melting begins in an axial segment, there are five constituents from which gas and volume may be moved into the molten cavity: (1) the initial central void, (2) the grain boundaries, (3) intragranular, (4) the as-fabricated porosity, and (5) the fuel cracks. Each of these can affect the molten cavity pressurization through the gas and volume associated with their inclusion.

39. Prior to melting, the central void is considered to be in equilibrium with the rest of the free volume within the pin. The number of moles of helium and fission gas associate with the central void in each axial segment varies depending on the volume, temperature, and pressure. The amount of this gas, therefore, changes during each time step throughout the pretransient and transient up to fuel melting initiation. Upon initial melting, the gas associated with the defined central molten cavity is fixed at its last value based on equilibrium with the plenum and associated free volume within the pin. This gas and its volume is then considered part of the molten cavity and is removed from the plenum pressure considera-

tions. It is implicitly assumed that melting initiates the production on a molten cavity region which acts as a bottle that does not communicated with the plenum.

40. The fission gas is assumed to exist in grain boundary bubbles that cause fuel swelling, and intra-granular gas within the fuel matrix. Upon fuel melting, the grain boundary gas and its volume is assumed to be released immediately into the molten cavity.

41. The intragranular gas is assumed to be tied-up in very small bubbles or interstitially located, so a time is required for the coalescence and buoyancy forces to release this gas into the cavity. Therefore, there can be gas in the molten fuel region which has not been released into the molten cavity. The intragranular gas is assumed to have no volume associated with it, so no volume movement occurs. The release of the gas retained within the molten fuel to the molten cavity through coalescence and buoyancy effects is assumed to occur at a rate proportional to the amount of gas present.

42. Like the grain boundary gas, the gas and volume associated with any residual as-fabricated porosity is assumed to be released to the molten cavity instantaneously upon melting. The same is true for any cracks in the cell and their associated gas and volume.

43. The discussion above covered the movement of gas and volume from various sources into the molten cavity. There are two other effects which will change the volume associated with the molten cavity: (1) fuel volume change on melting, and (2) molten fuel thermal expansion. Any changes due to swelling or contraction of the remaining grain boundary fission gas bubbles are treated in the fuel swelling routine.

44. DEFORM-4 contains a function routine which determines the theoretical density of the fuel at any given temperature. Since it is assumed that there is no mass transfer between radial cells or axial segments, the volume change for each cell can be determined. This density function includes both solid and molten fuel thermal expansion, as well as the transition between solid and molten fuel.

45. The molten cavity pressure is determined from the ideal gas law applied over the entire cavity. The number of moles of gas in the cavity is determined by adding the changes discussed above to the amount present at the start of the time step. The volume is similarly determined. It is assumed that the boundary between the outer most cell that is melting and the solid fuel remains stationary during the time step. While this is not necessarily true, appropriate choice of the transient time step length will provide a close link between cavity pressurization and mechanical response to this force without the need to iterate between the cavity pressure and mechanical response parts of the code.

46. Because of the volume changes occurring as a transient progresses, it is possible for the central void in an axial segment to completely close. The case may even exist where there is more volume needed than exists inside the solid boundary. Because DEFORM-4 does not provide for relocation of fuel between axial segments, the additional material cannot be moved. However, to at least study the pressurization effects, when this situation arises, a volume deficit is calculated. This is removed from the free volume to approximate the movement into available volume.

47. In addition to the pressure from the gases in the molten cavity, the fuel vapor pressure is included. The temperature used is the maximum radially-mass-averaged temperature over the axial extent of the cavity. In the case where each axial segment is a separate cavity, the mass-averaged temperature of the segment is used. The fuel vapor pressure terms are added to the gas-induced pressure to obtain the total molten cavity pressure.

FUEL-CLADDING GAP CONDUCTANCE

48. The thermal coupling between the cladding and the fuel is important because it affects the fuel and coolant temperatures and thereby, the swelling and thermal expansion of the fuel and cladding. The gap conductance provides this coupling. If the values are high, the fuel temperatures are lower, reducing the fuel swelling, thermal expansion, restructuring, fission-gas release, and stored energy. If the gap conductance is poor due to a large gap or a low conductivity gas mixture in the gap, then all fuel temperatures are raised, enhancing the phenomena mentioned previously. Because of the sensitivity of phenomena to temperature, and therefore gap conductance, it is best to describe the elements which contribute to the heat transfer between the fuel and cladding as mechanistically as possible. The gap conductance is determined at the end of each DEFORM-4 time step, and is used for the fuel-cladding thermal coupling when determining the temperatures at the end of the next time step.

49. The conductance is determined from three components: (1) radiative heat transfer between the fuel and cladding surfaces, (2) conduction heat transfer through the gas in a residual gas gap, and (3) solid-to-solid heat transfer where the gap is closed. The influences of interface pressure, surface roughnesses, gas composition, and fuel and cladding conductivities are all included. The total gap conductance is the sum of the three components.

PIN FAILURE

50. There are a number of methods that may be used in DEFORM-4 to determine pin failure and begin the failed pin modules. These include several calculated failure correlations and input conditions. Conditions such as time, temperature, or melt fraction may be specified as the failure initiator. Also available are biaxial stress rupture, transient burst temperature, Larson-Miller life fraction, and cladding strain criteria. There is a special option which uses a hoop stress criterion that is consistent with the rip propagation modeling in the failed fuel modules of the code.

51. All the failure criteria are cast into the form of a failure fraction that must mach one before failure occurs. In those criteria that yield a failure time or quantity (such as a

failure strain), this is divided into the incremented magnitude calculated during the time step yielding a failure fraction. This is then added to the previously accumulated values, until a value of one or greater is achieved. If this occurs, the fuel is checked to determine if it is fully cracked to the central void or the molten region. This fuel failure is also a necessary condition for failed fuel model initiation, so both the cladding and fuel must have failed. As failure is approached, the computational time step is reduced.

52. In the current version of SAS4A, once a failed fuel model is initiated, DEFORM-4 stops its calculations. Under current development is the capability for DEFORM-4 to be operational in unfailed axial segments concurrently with the failed fuel models thereby continuing the transient response of the fuel pin in a more mechanistic fashion.

53. One of the newest features to be incorporated into the DEFORM-4 is the ability to handle the fast creep of the cladding at elevated temperatures and high internal pressures when the fuel is fully cracked to the molten region. In this situation the consistency between cavity and interface pressure is maintained through appropriate governing equations and cladding strain. As the central cavity pressure builds within a solid fuel annulus, appreciable pressures can be produced, but once the fuel becomes fully cracked, the inclusion of additional volume through closing of the fuel-cladding gap or the inclusion of crack volume usually produces a drop in the cladding stress until future pressurization occurs. The creep of the cladding also introduces extra volume into the cavity that mitigates pressure buildup.

RESULTS AND VALIDATION

54. Previous papers have reported the initial calculations used to validate the results of DEFORM-4 against experimental data (Ref. 1 and 2). In both cases, DEFORM-4 produced steady state results that agreed well with sibiling pin data in the quantities of fission gas release, porosity distribution, grain size distribution and physical dimensions. Both LO3 and LO7 experiments used pins irradiated to about 3.5% average burnup.

55. Further slow ramp TOP validation calculations have been performed on the WHC/HEDL TREAT experiments TS-1 and TS-2 (Ref. 3). The TS-1 experiment used an 8 day irradiated pin while TS-2 used a pin irradiated to about 6%. The DEFORM-4 characterizations of these pins produced very good agreement with sibling pin data, giving additional assurance of DEFORM-4's ability to correctly characterize the pre-transient condition of the pins.

56. Because of the axial relocation that occurred in TS-1 and TS-2, and because the PINACLE module (Ref. 4) was not used in conjuction with DEFORM-4 for these calculations, a simple axial relocation model was implemented in the molten cavity routine that introduced the volume associated with insulator pellet movement.

57. In both simulated 5¢/s reactivity insertion transients, DEFORM-4 predicted the occurrance of the major events near their actual timing. Table 1 and 2 give a summary of these results. In addition, the predicted melt fractions and axial extent of failure were very close to the experimental observations. These results demonstrate the versatility of the DEFORM-4 module and its capability to produce reasonable predictions of accident scenarios and failure characteristics.

58. The influence of axial expansion assumptions on the transient results of a full reactor represented by 10 channels is shown in Fig. 3. This model represents a hypothetical homogeneous, two-batch recycle core with a high coolant void worth. This study was undertaken to observe the sensitivity of transient results to the assumed expansion mode because of the results obtained from analyses of experiments in RAPSODIE (Ref. 5). The free fuel expansion assumption produced a minimum normalized power of 0.685 at 17 seconds, the cladding expansion controlled assumption reached 0.523 at 21.17 seconds, and the force balance between fuel and cladding produced a normalized power of 0.644 at 18 seconds. Once boiling begins the power level rises rapidly. The peak power and times for the three assumptions is 1371 at 18.17 seconds 4640 at 22.58 seconds, and 2082 at 19.22 seconds, respectively (Fig. 3). The integrated energy (full power seconds) for the three cases were 29.11, 29.61, and 34.44 seconds, respectively. While the cladding controlled assumption makes the LOF phase of the transient more benign than the other cases, it increases the severity of the TOP phase significantly. These results indicate the need to understand more fully the actual modes of axial expansion present in the LOF and TOP scenarios.

59. Another result that developed from this study involved the failure predictions. DEFORM-4 models the situation of a molten central cavity and fully cracked fuel, as occurred in the TOP phase of the transient, and the resulting cladding stress state. In each of these cases, failure was initiated on a melt fraction

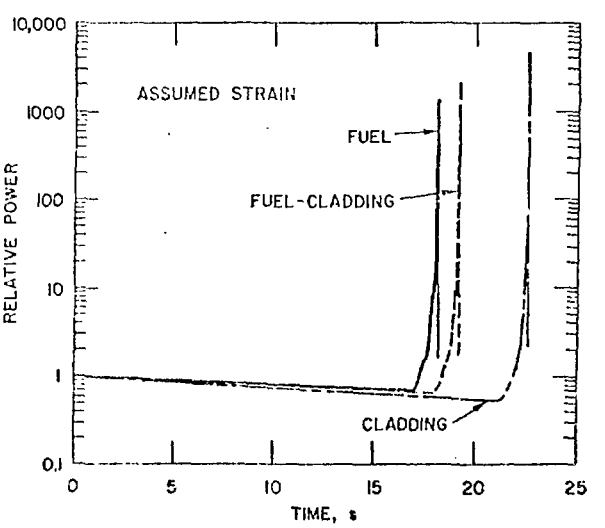

Fig. 3. Effects of Axial Expansion Assumption

Table 1

Comparison of TS-1 Observations with SAS4A/DEFORM-4 Predictions

Event	Observation	SAS4A/DEFORM-4
Fuel Melts	-	17.2 s*
Fuel Relocation	27.2 - 27.3 s	27.5 s
Rapid Cladding Straining	-	31.9 s
Fuel Pin Failure	32.2 s	$\geq$ 32.2 s
Location of Failure (X/L)	0.85 - 0.90	0.8 - 0.9

Table 2

Comparison of TS-2 Observations with SAS4A/DEFORM-4 Predictions

Event	Observation	SAS4A/DEFORM-4
Fuel Relocation	29.7 s	29.7 s*
Rapid Cladding Straining	-	32.0 s
Fuel Pin Failure	33.83 s	33.0 - 33.7 s
Location of Failure (X/L)	0.65 - 0.80	0.60 - 0.90

*All times in TREAT Time

basis, about the mechanics calculation does not predict failure of any of the pins at this time.

60. The new DEFORM-4 module is SAS4A has been developed to be a faster running code than previous versions and produce more mechanistic results. Validation studies to date demonstrate the appropriate of the approached used and other studies have shown the versatility of the code in studying specific phenomena and their affect on accident scenarios.

References

1. D. J. Hill, "SAS4A Validation and Analysis of In-Pile experiments for Slow Ramp TOP's," Proc. of the International topical Mtg. on Fast Reactor Sfety, vol. 2 p. 791, Knoxville, TN (April 21-25, 1985).

2. J. A. Morman et al., "SAS Validation and Analysis of In-Pile TUCOP Experiments," Proc. of the International Topical Mtg. on Fast Reactor Safety, Vol. 2 p. 797, Knoxville, TN (April 21-25, 1985).

3. A. L. Pitner et al., "TS-1 and TS-2 Transient Overpower Test on FFTF Fuel,"- Trans. Am. Nucl. Soc. 50, p. 351 (1985).

4. A. M. Tentner and D. J. Hill, "PINACLE-A Mechanistic Model for the Analysis of In-Pin Fuel Relocation Under LOF and TOP Conditions for SAS4A," Trans. Am. Nuc. Soc. 49 p. 275 (1985).

5. A. Languille et al., "Results of Tests Under Normal and Abnormal Operating Conditions Concerning LMFBR fuel Element Behavior," Proc. of the International Topical Mtg. on Fast Reactor Safety, Vol. 2 p. 667, Knoxville, TN (April 21-25, 1985).